

Figure S1 The image presents a sample echocardiographic image of the different types of views. The top row shows the two-dimensional echocardiograms, the second row is pulse Doppler images, and the bottom row is tissue Doppler images.

Table S1 Baseline characteristics of the training and validation dataset

Clinical characteristics	Training and internal validation dataset	Training dataset	Internal Validation dataset	External validation dataset
Case number	201	141	60	30
Video number	594	416	178	90
Image number	1,283	892	391	120
Age (year)	47.8±14.7	47.7±14.3	48.0±15.7	41.2±10.3
Gender (male)	103 (98)	74 (67)	29 (31)	17 (13)
Height (cm)	163.5±8.8	164.1±8.6	162.1±9.4	165.0±8.9
Weight (kg)	62.6±12.2	63.4±12.8	60.7±10.4	61.6±11.4
BSA (m ²)	1.67±0.19	1.69±0.19	1.64±0.16	1.67±0.17
Systolic pressure (mmHg)	131.2±22.5	130±21.6	133.1±24.6	110.2±24.3
Diastolic pressure (mmHg)	80.8±12.2	80.6±12.0	81.3±12.7	75.6±9.8
Heart rate (bpm)	71.3±11.7	71.8±11.8	70.3±11.3	71.2±10.8
LVEF (%)	67.8±6.0	68.5±5.7	66±6.5	65.0±7.5

Data are presented as mean ± standard deviation or n. BSA, body surface area; LVEF, left ventricular ejection fraction.

Table S2 Criteria for measurement of cardiac structural parameters in echocardiography video (4,21,24)

Parameters	Measurement criteria
End-diastole (ED)	End-diastole is defined as the first frame after mitral valve closure or the frame in the cardiac cycle in which the respective left ventricle (LV) dimension or volume measurement is the largest
End-systole (ES)	End-systole is defined as the frame after aortic valve closure or the frame in which the cardiac dimension or volume is smallest
Parasternal long-axis view (PLAX)	
AO-a	The anteroposterior diameter of the aortic annulus
AO-s	The maximal diameter of the aortic sinus is usually the midpoint
RVOT-Prox	The linear dimension was measured from the anterior right ventricle (RA) wall to the interventricular septal-aortic junction
LA-ap	The anteroposterior diameter of the left atrium (LA) can be measured perpendicular to the aortic root long axis, and measured at the level of the aortic sinuses by using the leading-edge to leading-edge convention
LV-ap	Linear internal measurements of the LV should be acquired from the parasternal approach carefully obtained perpendicular to the LV long axis, and measured at the level of the mitral valve leaflet tips
MV-ap	The diameter of the mitral annulus should be measured from the base of the posterior and anterior leaflets
Apical four-chamber view (A4C)	
LVID base-t	The maximal transversal dimension in the basal one-third of LV
LVID middle-t	The transversal LV diameter is in the middle third of LV, approximately halfway between the maximal basal diameter and the apex, at the level of papillary muscles
LVID-I	At the mitral valve level, connect the two opposite sections of the mitral ring with a straight line. LV length is defined as the distance between the bisector of this line and the apical point of the LV contour, which is most distant to it
LA-t	The LA-t was taken from a perpendicular constructed from the midpoint of the superoinferior dimension extending to the atrial borders
LA-I	LA length was defined by a line bisecting the LA extending from the midpoint of the mitral annulus to the midpoint of the superior (cephalad) LA border
RA-t	The dimension should be taken from a plane perpendicular to the long axis of the right atrium (RA), extending from the lateral border of the RA to the interatrial septum
RA-I	The maximal long-axis distance of the RA is from the center of the tricuspid annulus to the center of the superior RA wall, parallel to the interatrial septum
MV-t	The transversal diameter of the mitral annulus should be measured from the base of the posterior and anterior leaflets
TV-t	The transversal diameter of the tricuspid annulus should be measured from the base of the septal and anterior leaflets
Right ventricular apical four-chamber view (RV-A4C)	
RV-I	The longitudinal dimension is drawn from the plane of the tricuspid annulus to the RV apex
RV base-t	The maximal transversal dimension in the basal one-third of RV inflow in the RV-focused view
RV middle-t	The transversal RV diameter is in the middle third of RV inflow, approximately halfway between the maximal basal diameter and the apex, at the level of papillary muscles

Ao-a, diameter of aortic annulus; Ao-s, diameter of aortic sinus; LA-ap, anteroposterior dimension of the left atrium; LA-I, long-axis dimension of left atrium; LA-t, transverse dimension of left atrium; LVID base-t, basal transverse dimension of left ventricle; LVID middle-t, mid transverse dimension of left ventricle; LVID-ap, anteroposterior dimension of left ventricular; LVID-I, long-axis dimension of left ventricle; MV-ap, anteroposterior dimension of the mitral annulus; MV-t, transverse dimension of the mitral annulus; RA-I, long-axis dimension of right atrium; RA-t, transverse dimension of right atrium; RV base-t, basal transverse dimension of right ventricle; RV middle-t, mid transverse dimension of right ventricle; RV-I, long-axis dimension of right ventricle; RVOT-Prox, proximal dimension of right ventricular outflow tract; TV-t, transverse dimension of the tricuspid annulus.

Table S3 Measurement criteria for Doppler echocardiograms (4,9,25)

Parameters	Measurement criteria
Transvalvular velocity	When measuring velocities, use the outer edge of the dense (or bright) envelope of the spectral recording
Spectral tracing	When tracing the velocity to derive velocity-time integral (VTI), it is best to trace the outer edge of the densest (or brightest) portion of the spectral tracing (i.e., the modal velocity) and ignore the dispersion that occurs near peak velocity
E-wave and A-wave	E-wave is defined as the peak early filling, and A-wave is defined as late diastolic filling
Pulsed-wave DTI	The spectral longitudinal velocity of the myocardium normally consists of a positive systolic wave and two diastolic peaks, one during early diastole and a second during atrial contraction. The peak systolic annulus velocity has been expressed as S, the early diastolic annular velocity has been expressed as e', and the late diastolic velocity as a'

DTI, doppler tissue imaging.

Table S4 The SD ratio of Auto-Echo and human measurements in cardiac structure parameters

Parameters	SD ratio		
	Automated vs. Hunan experts	Moderately experienced reader vs. Hunan experts	Less experienced reader vs. Hunan experts
Ao-a (mm)	0.84	1.25	1.22
Ao-s (mm)	0.79	1.06	1.03
RVOT (mm)	0.97	1.09	1.06
LA-ap (mm)	0.81	0.97	1.03
LVID-ap (mm)	0.89	1.34	1.32
MV-ap (mm)	0.84	1.74	1.53
LVID base-t (mm)	0.85	1.01	1.05
LVID middle-t (mm)	0.80	1.10	1.30
LVID-I (mm)	0.83	1.27	1.51
LA-t (mm)	0.96	1.03	1.40
LA-I (mm)	0.83	1.00	1.14
RA-t (mm)	1.02	1.13	1.19
RA-I (mm)	0.88	1.02	1.33
MV-t (mm)	0.72	0.97	1.21
TV-t (mm)	0.82	1.19	1.20
RV base-t (mm)	0.70	0.94	0.96
RV middle-t (mm)	0.80	1.03	1.04
RV-I (mm)	0.82	1.05	1.22

Ao-a, diameter of aortic annulus; Ao-s, diameter of aortic sinus; ED, end-diastole; ES, end-systole; LA-ap, anteroposterior dimension of the left atrium; LA-I, long-axis dimension of left atrium; LA-t, transverse dimension of left atrium; LVID base-t, basal transverse dimension of left ventricle; LVID middle-t, mid transverse dimension of left ventricle; LVID-ap, anteroposterior dimension of left ventricular; LVID-I, long-axis dimension of left ventricle; MV-ap, anteroposterior dimension of the mitral annulus; MV-t, transverse dimension of the mitral annulus; RA-I, long-axis dimension of right atrium; RA-t, transverse dimension of right atrium; RV base-t, basal transverse dimension of right ventricle; RV middle-t, mid transverse dimension of right ventricle; RV-I, long-axis dimension of right ventricle; RVOT, right ventricular outflow tract; SD, the standard deviation; TV-t, transverse dimension of the tricuspid annulus.

Table S5 Result of the Auto-Echo performance for automatic measurement of cardiac structure parameters in the internal validation dataset

Parameters	ICC (AI + Experts)	ICC (Experts)	r	Bias (LOAs)	SD	Absolute error (absolute relative error, %)		
						50%	75%	90%
PLAX								
Ao-a (mm)	0.93	0.88	0.88	-0.4 (-2.8, 1.9)	1.2	0.8 (4.1)	1.5 (7.8)	2.0 (10.7)
Ao-s (mm)	0.97	0.95	0.96	0.3 (-2.0, 2.7)	1.2	0.7 (2.5)	1.2 (4.3)	1.8 (6.6)
RVOT (mm)	0.97	0.96	0.94	-0.7 (-4.7, 3.3)	2.0	1.3 (5.4)	2.5 (10.3)	3.7 (14.1)
LA-ap (mm)	0.98	0.96	0.97	-0.7 (-4.7, 3.3)	2.1	0.9 (3.2)	1.9 (7.1)	3.8 (13.6)
LVID-ap (mm)	0.98	0.97	0.95	-1.5 (-5.6, 2.6)	2.1	1.5 (3.6)	2.9 (7.7)	4.1 (11.2)
MV-ap (mm)	0.90	0.84	0.84	-0.6 (-4.0, 2.7)	1.7	1.2 (4.8)	2.1 (8.4)	3.1 (12.3)
A4C								
LVID base-t (mm)	0.95	0.92	0.92	1.8 (-3.6, 7.2)	2.8	1.9 (4.9)	3.2 (8.8)	5.7 (15.8)
LVID middle-t (mm)	0.96	0.93	0.94	1.9 (-3.6, 7.4)	2.8	2.2 (6.7)	3.3 (12.3)	4.7 (20.1)
LVID-l (mm)	0.98	0.96	0.97	1.3 (-3.7, 6.4)	2.6	2.2 (2.9)	3.6 (5.3)	4.6 (7.0)
LA-t (mm)	0.97	0.96	0.95	-0.6 (-6.8, 5.5)	3.2	1.7 (5.7)	2.9 (9.6)	5.1 (15.5)
LA-l (mm)	0.97	0.95	0.96	1.5 (-4.2, 7.2)	2.9	1.5 (3.2)	2.9 (7.2)	4.9 (12.7)
RA-t (mm)	0.94	0.92	0.82	0.7 (-5.6, 7.0)	3.2	1.5 (5.7)	2.7 (9.4)	4.4 (17.7)
RA-l (mm)	0.97	0.96	0.95	-0.1 (-5.5, 5.2)	2.7	1.3 (3.5)	2.5 (6.7)	3.8 (10.7)
MV-t (mm)	0.89	0.77	0.86	0.6 (-3.6, 4.8)	2.2	1.2 (4.4)	2.6 (8.2)	4.0 (13.6)
TV-t (mm)	0.91	0.85	0.81	-0.2 (-4.9, 4.5)	2.4	1.3 (5.4)	2.2 (9.2)	3.4 (15.2)
RV-A4C								
RV base-t (mm)	0.93	0.85	0.93	0.3 (-4.3, 4.8)	2.3	1.3 (6.0)	2.3 (9.5)	4.1 (15.0)
RV middle-t (mm)	0.92	0.85	0.88	0.6 (-4.8, 5.8)	2.7	1.7 (9.7)	2.9 (18.7)	4.4 (26.4)
RV-l (mm)	0.94	0.90	0.90	-0.0 (-9.2, 9.3)	4.6	2.8 (5.7)	5.2 (9.7)	7.6 (14.9)

A4C, apical four-chamber view; Ao-a, diameter of aortic annulus; Ao-s, diameter of aortic sinus; LA-ap, anteroposterior dimension of the left atrium; LA-l, long-axis dimension of left atrium; LA-t, transverse dimension of left atrium; LVID base-t, basal transverse dimension of left ventricle; LVID middle-t, mid transverse dimension of left ventricle; LVID-ap, anteroposterior dimension of left ventricular; LVID-l, long-axis dimension of left ventricle; MV-ap, anteroposterior dimension of the mitral annulus; MV-t, transverse dimension of the mitral annulus; PLAX, parasternal long-axis view; RA-l, long-axis dimension of right atrium; RA-t, transverse dimension of right atrium; RV base-t, basal transverse dimension of right ventricle; RV middle-t, mid transverse dimension of right ventricle; RV-A4C, right ventricle focused apical four-chamber view; RV-l, long-axis dimension of right ventricle; RVOT-Prox, proximal dimension of right ventricular outflow tract; TV-t, transverse dimension of the tricuspid annulus; ICC, intraclass correlation coefficient; LOAs, limits of agreement; SD, standard deviation.

Table S6 The absolute relative error based on Auto-Echo vs. doctors with different experiences for cardiac structure diameter, and effects of phase and image quality on the performance of Auto-Echo in the internal validation dataset

Absolute relative error (%)	Performance of Auto-Echo vs. doctors			Keyframe		Image quality	
	Auto-Echo	Moderately experienced doctor	Less experienced doctor	ED	ES	Good	Poor
PLAX							
Ao-a ^{†‡§}	4.1 (1.8–7.8)	5.5 (2.3–10.3)	7.1 (3.9–11.9)	3.7 (1.8–6.0)	4.9 (1.8–8.3)	4.0 (1.8–7.3)	5.8 (2.0–10.6)
Ao-s† [‡]	2.5 (1.2–4.3)	3.9 (2.0–6.9)	4.1 (1.8–7.6)	2.4 (1.0–4.9)	2.5 (1.2–3.6)	2.4 (1.3–4.0)	4.6 (0.6–6.8)
RVOT-Prox ^{†§}	5.4 (2.5–10.3)	6.0 (3.0–10.8)	7.6 (3.6–12.9)	4.2 (1.8–7.6)	7.1 ^{**} (2.6–13.2)	5.0 (2.2–10.2)	6.8 (3.0–10.8)
LA-ap ^{†§}	3.2 (1.8–7.1)	4.5 (2.3–8.2)	6.0 (2.9–10.9)	5.5 ^{**} (1.9–10.5)	2.5 (1.3–4.3)	3.2 (1.7–6.8)	5.7 (1.5–17.1)
LV-ap ^{†§}	3.6 (1.7–7.7)	4.7 (2.0–8.7)	6.6 (3.1–11.4)	2.9 (1.5–5.7)	5.9 ^{**} (2.7–9.7)	3.4 (1.8–7.4)	5.7 (1.7–12.9)
MV-ap ^{†‡§}	4.8 (1.9–8.4)	7.3 (3.1–12.4)	17.6 (8.6–29.8)	4.5 (2.2–8.9)	4.8 (1.6–8.3)	4.7 (1.9–8.3)	6.0 (1.6–22.0)
A4C							
LVID base-t ^{†‡}	4.9 (2.9–8.8)	6.9 (3.4–12.3)	8.1 (3.3–15.5)	4.7 (1.8–7.4)	5.4 (3.2–13.5)	5.2 (2.8–9.2)	4.7 (2.5–7.7)
LVID middle-t ^{†‡§}	6.7 (3.1–12.3)	8.6 (4.0–19.1)	12.3 (6.2–25.4)	6.4 (3.3–10.0)	7.0 (2.8–15.0)	6.2 (2.8–10.1)	8.0 (3.3–17.0)
LVID-l ^{†‡§}	2.9 (1.5–5.3)	3.8 (1.8–7.1)	7.0 (3.6–11.0)	2.4 (1.3–4.3)	3.9 ^{**} (1.6–6.5)	2.3 (1.3–4.6)	4.3 [¶] (1.9–6.6)
LA-t ^{†§}	5.7 (2.6–9.6)	6.8 (3.0–12.7)	10.0 (4.4–19.2)	7.2 ^{**} (3.2–11.7)	4.3 (2.1–8.5)	6.2 (3.1–10.5)	4.7 (2.1–8.7)
LA-l ^{†‡}	3.2 (1.5–7.2)	6.2 (2.8–11.5)	6.8 (3.2–11.9)	3.2 (1.2–8.1)	2.8 (1.6–7.0)	3.0 (1.5–7.4)	3.6 (1.5–7.8)
RA-t ^{†§}	5.7 (2.8–9.4)	6.7 (3.3–13.1)	10.2 (5.0–18.5)	6.2 (3.2–11.7)	5.2 (2.1–8.3)	5.8 (2.9–8.4)	5.5 (2.3–13.7)
RA-l ^{†‡§}	3.5 (1.4–6.7)	5.1 (1.9–10.1)	7.4 (3.4–12.3)	3.5 (1.2–7.5)	3.4 (1.4–6.0)	3.2 (1.1–6.1)	4.0 (1.9–8.7)
MV-t ^{†‡§}	4.4 (2.3–8.2)	6.9 (3.6–12.3)	9.8 (4.7–16.4)	4.4 (2.5–7.7)	4.6 (2.1–9.1)	4.0 (2.0–8.0)	5.2 (2.7–9.1)
TV-t ^{†‡§}	5.4 (2.3–9.2)	9.3 (4.4–15.1)	14.0 (6.3–23.3)	5.3 (2.3–7.7)	5.4 (2.2–13.9)	5.3 (2.5–8.3)	6.1 (2.1–12.7)
RV-A4C							
RV base-t ^{†‡}	6.0 (3.0–9.5)	10.0 (4.9–19.4)	11.4 (5.6–21.6)	4.4 (2.7–9.1)	7.5 ^{**} (3.4–12.0)	5.7 (2.6–9.3)	6.6 (3.4–11.9)
RV middle-t ^{†‡}	9.7 (3.7–18.7)	18.6 (9.8–31.1)	18.5 (9.3–35.7)	8.3 (2.8–14.2)	11.2 ^{**} (5.7–22.4)	7.9 (3.4–16.6)	13.1 [¶] (6.6–24.4)
RV-l ^{†‡§}	5.7 (2.7–9.7)	9.0 (4.4–14.7)	13.2 (6.5–22.3)	6.6 (2.3–10.3)	5.6 (2.7–9.0)	6.5 (2.9–10.7)	5.7 (1.0–9.2)

Data are presented as median (interquartile range, IQR). Kruskal-Wallis test was used to compare the relative error between Auto-Echo and doctors with different experiences, and the Bonferroni test was used for subsequent pairwise comparisons. [†], difference in relative error between Auto-Echo and moderately experienced doctors values. [‡], difference in relative error between Auto-Echo and less experienced doctors values. [§], difference in relative error between moderately experienced doctors and less experienced doctors values. Subgroup analysis between two groups was performed using the Wilcoxon signed-rank test. ^{**}, difference in relative error between ED frame and ES frame values. [¶], difference in relative error between good image quality and bad image quality. A4C, apical four-chamber view; Ao-a, diameter of aortic annulus; Ao-s, diameter of aortic sinus; ED, end-diastole; ES, end-systole; LA-ap, anteroposterior dimension of the left atrium; LA-l, long-axis dimension of left atrium; LA-t, transverse dimension of left atrium; LVID base-t, basal transverse dimension of left ventricle; LVID middle-t, mid transverse dimension of left ventricle; LVID-ap, anteroposterior dimension of left ventricular; LVID-l, long-axis dimension of left ventricle; MV-ap, anteroposterior dimension of the mitral annulus; MV-t, transverse dimension of the mitral annulus; PLAX, parasternal long-axis view; RA-l, long-axis dimension of right atrium; RA-t, transverse dimension of right atrium; RV base-t, basal transverse dimension of right ventricle; RV middle-t, mid transverse dimension of right ventricle; RV-A4C, right ventricle focused apical four-chamber view; RV-l, long-axis dimension of right ventricle; RVOT-Prox, proximal dimension of right ventricular outflow tract; TV-t, transverse dimension of the tricuspid annulus.

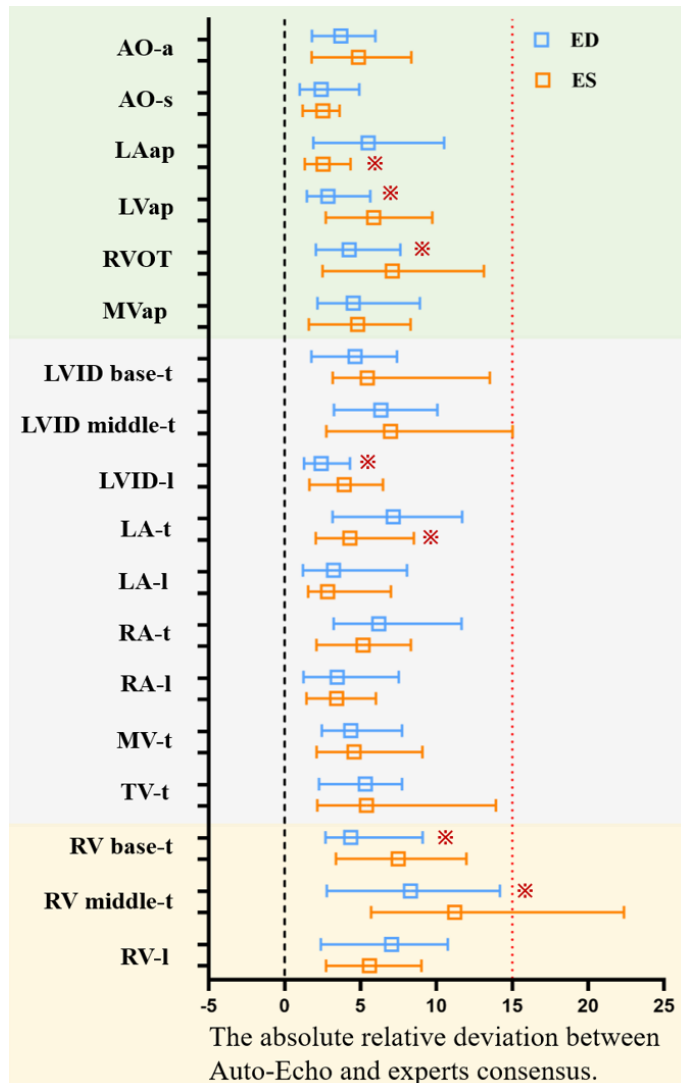


Figure S2 Subgroup analysis of Auto-Echo performance in clinically relevant frames. The absolute relative deviations between Auto-Echo measurements and expert consensus in the end-diastole frame (blue) and end-systole frame (orange). *, difference in the Auto-Echo performance between ED and ES frame. Ao-a, diameter of aortic annulus; Ao-s, diameter of aortic sinus; ED, end-diastole; ES, end-systole; LA-ap, anteroposterior dimension of the left atrium; LA-l, long-axis dimension of left atrium; LA-t, transverse dimension of left atrium; LVID base-t, basal transverse dimension of left ventricle; LVID middle-t, mid transverse dimension of left ventricle; LVID-ap, anteroposterior dimension of left ventricular; LVID-l, long-axis dimension of left ventricle; MV-ap, anteroposterior dimension of the mitral annulus; MV-t, transverse dimension of the mitral annulus; RA-l, long-axis dimension of right atrium; RA-t, transverse dimension of right atrium; RV base-t, basal transverse dimension of right ventricle; RV middle-t, mid transverse dimension of right ventricle; RV-I, long-axis dimension of right ventricle; RVOT, right ventricular outflow tract; TV-t, transverse dimension of the tricuspid annulus.

Table S7 Result of the Auto-Echo performance for automatic measurement of cardiac structure parameters in the external validation dataset

Parameters	ICC	r	Bias (LOAs)	SD	Absolute error (absolute relative error, %)		
					50%	75%	90%
PLAX							
Ao-a (mm)	0.83	0.78	0.0 (-2.7, 2.7)	1.4	0.9 (4.4)	1.3 (6.6)	2.3 (10.5)
Ao-s (mm)	0.88	0.79	0.5 (-3.5, 2.6)	1.6	0.9 (3.6)	1.5 (5.2)	2.3 (9.3)
RVOT (mm)	0.95	0.92	-1.1 (-4.9, 2.6)	1.9	1.4 (6.0)	2.3 (10.4)	3.4 (15.6)
LA-ap (mm)	0.98	0.96	-0.6 (-3.7, 2.5)	1.6	1.0 (4.3)	1.8 (6.8)	2.6 (9.7)
LVID-ap (mm)	0.96	0.92	0.8 (-5.2, 6.9)	3.1	2.5 (6.5)	3.7 (12.4)	5.0 (17.2)
MV-ap (mm)	0.78	0.63	-1.8 (-6.1, 2.5)	2.2	2.1 (8.5)	3.3 (12.6)	5.0 (17.3)
A4C							
LVID base-t (mm)	0.93	0.86	-1.1 (-6.2, 4.1)	2.6	1.5 (4.1)	2.8 (6.5)	5.6 (15.1)
LVID middle-t (mm)	0.92	0.85	-1.1 (-8.3, 6.1)	3.7	2.3 (7.6)	4.1 (12.7)	6.7 (22.2)
LVID-I (mm)	0.95	0.91	4.4 (-2.6, 11.4)	3.6	4.7 (7.6)	6.5 (9.9)	8.9 (13.5)
LA-t (mm)	0.95	0.91	-0.7 (-6.1, 4.6)	2.7	1.6 (5.5)	3.5 (12.6)	4.4 (17.9)
LA-I (mm)	0.98	0.96	-1.7 (-5.7, 2.2)	2.0	2.0 (4.2)	3.3 (7.0)	4.7 (10.2)
RA-t (mm)	0.93	0.87	-0.7 (-5.9, 4.5)	2.7	1.7 (5.3)	3.1 (9.2)	4.5 (14.0)
RA-I (mm)	0.97	0.93	-0.8 (-6.5, 5.0)	2.9	1.9 (4.6)	3.1 (7.9)	4.6 (11.9)
MV-t (mm)	0.76	0.62	0.2 (-4.2, 4.6)	2.2	1.3 (5.0)	2.4 (8.6)	3.7 (13.7)
TV-t (mm)	0.69	0.53	2.2 (-5.4, 9.8)	3.9	2.3 (9.9)	3.5 (16.3)	6.5 (25.4)
RV-A4C							
RV base-t (mm)	0.87	0.78	-2.5 (-8.5, 3.5)	3.1	2.8 (12.5)	4.6 (17.6)	6.8 (24.2)
RV middle-t (mm)	0.95	0.91	2.2 (-6.4, 10.9)	4.4	3.6 (6.4)	5.5 (10.8)	7.9 (16.3)
RV-I (mm)	0.89	0.82	-1.1 (-7.2, 5.1)	3.1	1.9 (6.8)	3.4 (12.1)	4.9 (14.6)

A4C, apical four-chamber view; Ao-a, diameter of aortic annulus; Ao-s, diameter of aortic sinus; LA-ap, anteroposterior dimension of the left atrium; LA-I, long-axis dimension of left atrium; LA-t, transverse dimension of left atrium; LVID base-t, basal transverse dimension of left ventricle; LVID middle-t, mid transverse dimension of left ventricle; LVID-ap, anteroposterior dimension of left ventricular; LVID-I, long-axis dimension of left ventricle; MV-ap, anteroposterior dimension of the mitral annulus; MV-t, transverse dimension of the mitral annulus; PLAX, parasternal long-axis view; RA-I, long-axis dimension of right atrium; RA-t, transverse dimension of right atrium; RV base-t, basal transverse dimension of right ventricle; RV middle-t, mid transverse dimension of right ventricle; RV-I, long-axis dimension of right ventricle; RVOT-Prox, proximal dimension of right ventricular outflow tract; TV-t, transverse dimension of the tricuspid annulus; ICC, intraclass correlation coefficient; LOAs, limits of agreement; SD, standard deviation.

Table S8 The SD ratio of Auto-Doppler and human measurements in cardiac function parameters in the internal validation dataset

Parameters	SD ratio		
	Automated vs. Hunan experts	Moderately experienced reader vs. Hunan experts	Less experienced reader vs. Hunan experts
AV_Vmax (cm/s)	1.39	1.13	1.50
AV_Vmean (cm/s)	1.09	1.05	1.27
AV_VTI (cm)	1.02	1.09	1.37
LVET (ms)	1.00	1.19	1.41
PV_Vmax (cm/s)	1.02	0.85	1.14
PV_Vmean (cm/s)	0.95	0.91	1.03
PV_VTI (cm)	1.11	1.42	1.75
RVET (ms)	0.88	1.15	1.47
MV-E (cm/s)	0.98	1.18	2.23
MV-A (cm/s)	0.83	1.00	1.53
MV_E/A	0.69	1.31	1.76
MV_Vmax (cm/s)	1.05	1.17	1.28
MV_Vmean (cm/s)	0.86	1.13	1.13
MV_VTI (cm)	0.84	1.42	1.34
LVDFT (ms)	0.77	1.29	1.16
TV-E (cm/s)	1.20	1.40	2.14
TV-A (cm/s)	0.66	0.78	0.94
TV_Vmax (cm/s)	0.89	0.97	1.33
TV_Vmean (cm/s)	0.98	1.13	1.16
TV_VTI (cm)	0.81	1.68	1.71
RVDFT (ms)	0.94	2.01	2.15
MVS_S (cm/s)	0.64	1.06	1.10
MVS_e' (cm/s)	1.08	1.27	1.47
MVS_a' (cm/s)	1.90	1.76	1.55
MVL_S (cm/s)	0.69	1.29	1.40
MVL_e' (cm/s)	0.61	1.45	1.10
MVL_a' (cm/s)	0.78	1.69	1.44
TVL_S (cm/s)	0.79	1.15	1.48
TVL_e' (cm/s)	0.91	1.69	1.79
TVL_a' (cm/s)	1.56	1.47	1.90

AV, aortic valve; LVDFT left ventricular diastolic filling time; LVET, left ventricular ejection time; MV, mitral valve; MVL, mitral valve lateral; MVS, mitral valve septal; PV, pulmonary valve; RVDFT, right ventricular diastolic filling time; RVET, right ventricular ejection time; TV, tricuspid valve; TVL, tricuspid valve lateral; VTI, velocity-time integral.

Table S9 Result of the Auto-Doppler performance for automatic measurement of Doppler parameters in the internal validation dataset

Parameters	ICC (AI + Experts)	ICC (Experts)	r	Bias (LOAs)	SD	Absolute error (absolute relative error, %)		
						50%	75%	90%
AVPW								
Vmax (cm/s)	0.99	0.99	0.98	-1.9 (-11.3, 7.5)	4.8	3.1 (2.8)	5.7 (4.8)	8.3 (7.2)
Vmean (cm/s)	0.99	0.98	0.96	0.4 (-7.5, 8.4)	4.1	2.2 (3.1)	4.3 (6.4)	6.5 (8.7)
VTI (cm)	0.95	0.94	0.94	-2.0 (-6.7, 2.6)	2.4	1.9 (8.3)	3.2 (11.8)	4.1 (16.5)
LVET (ms)	0.88	0.85	0.84	-14.8 (-50.9, 21.3)	18.4	15.6 (4.5)	22.6 (7.0)	34.7 (10.7)
PVPW								
Vmax (cm/s)	0.98	0.96	0.96	-0.0 (-8.8, 8.7)	4.5	2.4 (2.7)	5.1 (5.6)	7.0 (8.2)
Vmean (cm/s)	0.97	0.95	0.92	-0.6 (-7.8, 6.6)	3.7	1.9 (3.4)	4.1 (6.7)	6.9 (11.3)
VTI (cm)	0.94	0.91	0.92	-0.7 (-4.6, 3.2)	2.0	1.2 (7.5)	2.7 (14.8)	3.3 (19.2)
RVET (ms)	0.90	0.85	0.81	-4.3 (-43.5, 35.0)	20.0	13.9 (4.2)	26.0 (8.6)	33.0 (10.5)
MVPW								
MV-E (cm/s)	0.99	0.99	0.99	-0.5 (-7.5, 6.5)	3.6	2.1 (2.9)	3.5 (5.0)	4.8 (8.9)
MV-A (cm/s)	0.99	0.98	0.99	0.0 (-9.3, 9.3)	4.7	1.9 (2.8)	3.5 (5.4)	8.5 (10.3)
E/A	0.99	0.97	0.99	0.0 (-0.2, 0.2)	0.1	0.0 (2.7)	0.1 (6.9)	0.1 (8.9)
Vmax (cm/s)	0.99	0.99	0.99	0.4 (-7.6, 8.4)	4.1	2.0 (2.4)	3.6 (4.0)	6.5 (8.0)
Vmean (cm/s)	0.99	0.98	0.99	-1.6 (-5.7, 2.4)	2.1	2.1 (5.2)	3.2 (7.0)	4.9 (11.9)
VTI (cm)	0.97	0.95	0.93	-0.9 (-7.4, 5.5)	3.3	2.0 (8.6)	4.0 (16.9)	5.1 (24.1)
LVDFT (ms)	0.98	0.96	0.97	0.3 (-60.9, 61.4)	31.2	22.6 (4.9)	30.5 (7.9)	46.9 (10.6)
TVPW								
TV-E (cm/s)	0.97	0.97	0.93	-0.9 (-8.5, 6.7)	3.9	2.4 (5.4)	4.9 (11.6)	6.7 (18.3)
TV-A (cm/s)	0.97	0.94	0.97	0.9 (-5.1, 6.9)	3.1	1.7 (5.4)	3.6 (8.2)	6.2 (13.9)
Vmax (cm/s)	0.97	0.95	0.94	0.0 (-7.0, 6.9)	3.5	2.1 (4.3)	4.2 (6.9)	6.5 (13.9)
Vmean (cm/s)	0.97	0.96	0.94	-1.1 (-5.5, 3.2)	2.2	1.9 (6.1)	2.7 (10.7)	4.1 (16.4)
VTI (cm)	0.96	0.93	0.94	-0.3 (-4.4, 3.8)	2.1	1.3 (8.3)	2.7 (15.5)	3.7 (24.6)
RVDFT (ms)	0.98	0.97	0.96	3.2 (-52.8, 59.3)	28.6	22.6 (4.2)	33.9 (7.4)	53.8 (9.4)
MVS-DTI								
s' (cm/s)	0.97	0.93	0.98	0.02 (-0.54, 0.57)	0.28	0.17 (2.5)	0.28 (4.1)	0.42 (5.8)
e' (cm/s)	0.99	0.99	0.98	0.29 (-0.71, 1.29)	0.51	0.33 (4.6)	0.45 (7.6)	0.76 (11.3)
a' (cm/s)	0.97	0.98	0.89	-0.02 (-1.82, 1.78)	0.92	0.24 (3.7)	0.59 (7.8)	1.33 (14.5)
MVL-DTI								
s' (cm/s)	0.99	0.97	0.97	0.05 (-0.63, 0.74)	0.35	0.16 (2.2)	0.34 (4.6)	0.66 (7.2)
e' (cm/s)	0.99	0.98	0.99	0.30 (-0.42, 1.02)	0.37	0.32 (4.0)	0.50 (6.2)	0.79 (10.5)
a' (cm/s)	0.98	0.97	0.98	0.03 (-0.99, 1.06)	0.52	0.22 (2.3)	0.33 (4.0)	0.59 (6.0)
TVL-DTI								
s' (cm/s)	0.98	0.96	0.97	0.16 (-0.59, 0.90)	0.38	0.20 (1.6)	0.37 (2.8)	0.61 (5.3)
e' (cm/s)	0.98	0.97	0.97	0.36 (-0.99, 1.72)	0.69	0.39 (3.8)	0.80 (8.0)	1.06 (15.1)
a' (cm/s)	0.97	0.98	0.90	0.00 (-2.27, 2.27)	1.16	0.29 (2.8)	0.56 (5.5)	1.7 (14.0)

AVPW, aortic valve-pulse wave; a', the peak late diastolic velocity of valve annulus by pulsed-wave DTI; E/A, the ratio of the peak late diastolic filling velocity to the peak early filling velocity; e', Peak early diastolic velocity of valve annulus by pulsed-wave DTI; LVDFT, left ventricular diastolic filling time; LVET, left ventricular ejection time; MVA, the peak early filling velocity of mitral inflow; MVE, the peak late diastolic filling velocity of mitral inflow; MVL-DTI, the Lateral side of the mitral annulus by pulsed-wave DTI; MVPW, mitral valve-pulse wave; MVS-DTI, the septal side of the mitral annulus by pulsed-wave DTI; PVPW, pulmonary valve-pulse wave; RVDFT, right ventricular diastolic filling time; RVET, right ventricular ejection time; S, Peak systolic velocity of valve annulus by pulsed-wave DTI; TVA, the peak early filling velocity of tricuspid inflow; TVE, the peak early filling velocity of tricuspid inflow; TVL-DTI, tricuspid annulus by pulsed-wave DTI; TVPW, tricuspid valve-pulse wave; Vmax, peak transvalvular velocity; Vmean, mean transvalvular velocity; VTI, velocity-time integral; ICC, intraclass correlation coefficient; LOAs, limits of agreement; SD, standard deviation.

Table S10 The absolute relative error based on Auto-Doppler *vs.* doctors with different experiences for Doppler parameter measurement in the internal validation dataset

Absolute relative error (%)	Auto-Doppler	Moderately experienced doctor	Less experienced doctor
AVPW			
Vmax (m/s) [§]	2.8 (1.3–4.8)	1.9 (0.9–3.8)	2.9 (1.5–6.0)
Vmean (m/s) ^{†‡}	3.1 (1.9–6.4)	3.1 (1.5–5.8)	5.4 (2.9–8.8)
VTI (cm) ^{†§‡}	8.3 (3.7–11.8)	9.4 (5.2–15.0)	14.8 (7.7–23.8)
LVET [‡]	4.5 (2.3–7.0)	5.2 (2.5–9.3)	8.4 (4.3–13.7)
PVPW			
Vmax (m/s) ^{†‡}	2.7 (1.7–5.6)	3.2 (1.5–6.4)	5.2 (2.7–8.4)
Vmean (m/s) ^{†‡}	3.4 (1.2–6.7)	3.7 (1.4–6.7)	5.7 (2.6–9.1)
VTI (cm) ^{†§‡}	7.5 (4.3–14.8)	11.9 (5.0–22.9)	20.2 (9.1–34.1)
RVET ^{†‡}	4.2 (2.2–8.6)	6.2 (2.9–12.7)	10.3 (4.7–18.2)
MVPW			
MVE (m/s) ^{†‡}	2.9 (1.0–5.0)	3.9 (2.2–7.0)	5.3 (2.2–8.9)
MVA (m/s) ^{‡§}	2.8 (1.1–5.4)	3.8 (2.0–8.1)	5.3 (2.6–11.5)
E/A [‡]	2.7 (0.9–6.9)	3.6 (1.7–6.4)	4.4 (2.0–10.0)
Vmax (m/s) ^{†‡}	2.4 (0.8–4.0)	3.4 (1.8–6.4)	4.2 (1.9–7.6)
Vmean (m/s)	5.2 (1.8–7.0)	4.7 (1.8–8.9)	5.0 (2.6–10.1)
VTI (cm) ^{†‡}	8.3 (5.1–16.9)	17.4 (7.4–32.8)	17.0 (8.8–31.1)
LVDFT [†]	4.9 (2.8–7.9)	7.2 (3.4–14.5)	6.5 (2.9–11.7)
TVPW			
TVE (m/s)	5.4 (2.2–11.6)	5.7 (2.5–10.2)	7.0 (3.5–12.4)
TVA (m/s) ^{‡§}	5.4 (1.6–8.2)	5.0 (1.9–11.2)	7.8 (4.5–13.7)
Vmax (m/s) [‡]	4.3 (1.7–6.9)	4.8 (2.0–9.1)	5.7 (3.5–10.4)
Vmean (m/s)	6.1 (2.5–10.7)	5.2 (2.7–10.9)	8.1 (3.5–14.0)
VTI (cm) ^{†‡}	8.3 (2.6–15.5)	22.5 (10.0–34.9)	22.0 (11.8–41.5)
RVDFT ^{†‡}	4.2 (2.1–7.4)	7.7 (3.3–13.4)	7.0 (2.4–15.0)
MVS-DTI			
S ^{†‡}	2.5 (1.2–4.1)	3.9 (1.8–6.8)	4.8 (2.2–8.8)
e'	4.6 (2.0–7.6)	3.7 (1.4–8.6)	4.7 (2.0–10.2)
a'	3.7 (1.8–7.8)	4.2 (1.7–8.6)	4.7 (2.5–8.0)
MVL-DTI			
S ^{†‡}	2.2 (0.6–4.6)	4.2 (2.0–8.0)	4.0 (1.7–8.6)
e'	4.0 (2.0–6.2)	4.0 (1.7–9.8)	4.7 (2.5–9.0)
a' ^{†‡}	2.3 (1.2–4.0)	4.8 (1.8–8.2)	4.3 (1.7–8.6)
TVL-DTI			
S ^{†‡}	1.6 (0.7–2.8)	4.1 (1.9–7.6)	4.3 (1.8–7.6)
e'	3.8 (2.4–8.0)	5.2 (2.4–11.1)	6.1 (2.6–12.5)
a' ^{‡§}	2.8 (1.0–5.5)	3.1 (1.4–6.9)	4.7 (2.4–9.3)

Data are presented as median (interquartile range, IQR). Kruskal-Wallis test was used to compare the relative error between Auto-Doppler and doctors with different years of experience, and the Bonferroni test was used for subsequent pairwise comparisons. [†], difference in relative error between Auto-Doppler and moderately experienced doctors values. [‡], difference in relative error between Auto-Doppler and less experienced doctors' values. [§], difference in relative error between moderately experienced doctors and less experienced doctors values. AVPW, aortic valve-pulse wave; a', the peak late diastolic velocity of valve annulus by pulsed-wave DTI; E/A, the ratio of the peak late diastolic filling velocity to the peak early filling velocity; e', Peak early diastolic velocity of valve annulus by pulsed-wave DTI; LVDFT, left ventricular diastolic filling time; LVET, left ventricular ejection time; MVA, the peak early filling velocity of mitral inflow; MVE, the peak late diastolic filling velocity of mitral inflow; MVL-DTI, the Lateral side of the mitral annulus by pulsed-wave DTI; MVPW, mitral valve-pulse wave; MVS-DTI, the septal side of the mitral annulus by pulsed-wave DTI; PVPW, pulmonary valve-pulse wave; RVDFT, right ventricular diastolic filling time; RVET, right ventricular ejection time; S, Peak systolic velocity of valve annulus by pulsed-wave DTI; TVA, the peak early filling velocity of tricuspid inflow; TVE, the peak early filling velocity of tricuspid inflow; TVL-DTI, tricuspid annulus by pulsed-wave DTI; TVPW, tricuspid valve-pulse wave; Vmax, peak transvalvular velocity; Vmean, mean transvalvular velocity; VTI, velocity-time integral.

Table S11 Result of the Auto-Doppler performance for automatic measurement of Doppler parameters in the external validation dataset

Parameters	ICC	r	Bias (LOAs)	SD	Absolute error (absolute relative error, %)		
					50%	75%	90%
AVPW							
Vmax (cm/s)	0.98	0.97	-0.9 (-11.4, 9.5)	5.3	2.7 (2.2)	5.6 (4.2)	9.1 (7.0)
Vmean (cm/s)	0.97	0.95	4.0 (-4.3, 12.3)	4.2	4.7 (6.4)	6.8 (9.0)	9.1 (11.6)
VTI (cm)	0.99	0.99	-1.3 (-4.1, 1.5)	1.4	1.1 (5.0)	2.1 (8.2)	3.0 (12.2)
LVET (ms)	0.96	0.93	-28.2 (-62.5, 6.0)	17.5	27.5 (9.3)	40.8 (13.1)	47.2 (15.6)
PVPW							
Vmax (cm/s)	0.98	0.94	0.0 (-8.0, 8.0)	4.1	3.4 (3.3)	4.2 (5.4)	6.5 (7.1)
Vmean (cm/s)	0.97	0.94	-1.4 (-7.9, 5.0)	3.3	2.4 (3.9)	4.0 (6.9)	5.8 (9.9)
VTI (cm)	0.97	0.92	-1.5 (-3.9, 1.0)	1.2	1.0 (7.6)	2.5 (15.7)	3.2 (17.0)
RVET (ms)	0.93	0.85	-18.3 (-55.3, 18.7)	18.9	15.9 (6.2)	32.6 (13.4)	43.7 (14.7)
MVPW							
MVE (cm/s)	0.98	0.96	-3.1 (-12.4, 6.2)	4.8	2.5 (2.5)	3.8 (4.1)	7.4 (8.6)
MVA (cm/s)	0.96	0.93	-4.6 (-19.4, 10.2)	7.5	3.3 (4.7)	5.2 (8.3)	13.7 (19.4)
E/A	0.86	0.93	0.2 (-1.4, 1.8)	0.8	0.07 (4.5)	0.13 (9.0)	0.27 (33.6)
Vmax (cm/s)	0.99	0.98	-2.2 (-7.9, 3.5)	2.9	2.1 (2.5)	3.6 (3.8)	5.9 (6.0)
Vmean (cm/s)	0.98	0.96	0.9 (-4.5, 6.4)	2.8	2.2 (4.6)	3.2 (6.8)	5.7 (12.3)
VTI (cm)	0.98	0.94	0.1 (-3.3, 3.4)	1.7	0.9 (5.2)	1.6 (8.7)	3.2 (16.7)
LVDFT (ms)	0.95	0.91	-9.7 (-84.4, 64.9)	38.1	17.7 (3.9)	27.3 (6.2)	52.0 (12.5)
TVPW							
TVE (cm/s)	0.98	0.97	-1.7 (-7.5, 4.2)	3.0	1.9 (3.0)	3.5 (5.4)	6.2 (10.6)
TVA (cm/s)	0.90	0.73	-4.0 (-14.2, 6.3)	5.2	3.4 (8.5)	5.9 (13.1)	9.7 (21.0)
Vmax (cm/s)	0.98	0.97	-1.7 (-7.5, 4.2)	2.3	1.9 (3.0)	3.5 (5.4)	6.2 (10.6)
Vmean (cm/s)	0.96	0.91	-0.4 (-5.0, 4.1)	2.3	1.3 (5.3)	2.5 (6.9)	3.6 (10.4)
VTI (cm)	0.94	0.90	-1.0 (-4.1, 2.1)	1.6	1.2 (9.0)	1.7 (11.8)	2.8 (19.2)
RVDFT (ms)	0.98	0.95	-24.5 (-66.9, 17.8)	21.6	25.4 (6.0)	35.4 (8.4)	58.1 (10.6)

AV, aortic valve; LVDFT left ventricular diastolic filling time; LVET, left ventricular ejection time; MV, mitral valve; PV, pulmonary valve; RVDFT, right ventricular diastolic filling time; RVET, right ventricular ejection time; TV, tricuspid valve; VTI, velocity-time integral; ICC, intraclass correlation coefficient; LOAs, limits of agreement; SD, standard deviation.